Clin Orthop Relat Res (2018) 476:1324-1338
DOI 10.1097/01.blo.0000534692.41467.02

Clinical Orthopaedics and Related Research®
A Publication of The Association of Bone and Joint Surgeons®

Basic Research

OPEN

Vitamin E Phosphate Coating Stimulates Bone Deposition in Implant-related Infections in a Rat Model

Arianna B. Lovati DVM, PhD, Marta Bottagisio MSc, Susanna Maraldi MD, Martina B. Violatto PhD, Monica Bortolin PhD, Elena De Vecchi PhD, Paolo Bigini PhD, Lorenzo Drago MD, Carlo L. Romanò MD

Received: 6 October 2007 / Accepted: 21 February 2018 / Published online: 16 May 2018

Abstract

Background Implant-related infections are associated with impaired bone healing and osseointegration. In vitro antiadhesive and antibacterial properties and in vivo anti-inflammatory effects protecting against bone loss of various formulations of vitamin E have been demonstrated in animal models. However, to the best of our knowledge, no in vivo studies have demonstrated the synergistic activity of vitamin E in preventing bacterial adhesion to orthopaedic implants, thus supporting the bone-implant integration.

Questions/purposes The purpose of this study was to test whether a vitamin E phosphate coating on titanium implants may be able to reduce (1) the bacterial colonization of prosthetic implants and (2) bone resorption and osteomyelitis in a rat model of *Staphylococcus aureus*-induced implant-related infection.

Methods Twelve rats were bilaterally injected in the femurs with *S aureus* UAMS-1-Xen40 and implanted with uncoated or vitamin E phosphate-coated titanium Kirschner wires without local or systemic antibiotic prophylaxis.

The institution of one or more of the authors (CLR) has received, during the study period, funding from the Italian Ministry of Health (# RC 2016, L4085).
Clinical Orthopaedics and Related Research® neither advocates nor endorses the use of any treatment, drug, or device. Readers are encouraged to always seek additional information, including FDA approval status, of any drug or device before clinical use.
Each author certifies that his or her institution approved the animal protocol for this investigation and that all investigations were conducted in conformity with ethical principles of research.
The in vivo analyses of this work were performed at the animal facility of the IRCCS Istituto di Ricerche Farmacologiche Mario Negri, Milan, Italy, and the ex vivo analyses at the IRCCS Galeazzi Orthopaedic Institute, Milan, Italy.
Two of the authors (LD, CLR) contributed equally.

A. B. Lovati, M. Bottagisio, Cell and Tissue Engineering Laboratory, IRCCS Galeazzi Orthopaedic Institute, Milan, Italy

S. Maraldi, C. L. Romanò, Dipartimento di Chirurgia Ricostruttiva e delle Infezioni Osteo-articolari, IRCCS Galeazzi Orthopaedic Institute, Milan, Italy

M. B. Violatto, P. Bigini, Nanobiology Unit, IRCCS Istituto di Ricerche Farmacologiche Mario Negri, Milan, Italy

M. Bortolin, E. De Vecchi, L. Drago, Laboratory of Clinical Chemistry and Microbiology, IRCCS Galeazzi Orthopaedic Institute, Milan, Italy

L. Drago, Department of Biomedical Science for Health, University of Milan, Milan, Italy

A. B. Lovati (✉), Cell and Tissue Engineering Laboratory, IRCCS Galeazzi Orthopaedic Institute, Via R. Galeazzi 4, 20161 Milan, Italy, email: arianna.lovati@grupposandonato.it

All ICMJE Conflict of Interest Forms for authors and *Clinical Orthopaedics and Related Research*® editors and board members are on file with the publication and can be viewed on request.

Eight rats represented the uninfected control group. A few hours after surgery, two control and three infected animals died as a result of unexpected complications. With the remaining rats, we assessed the presence of bacterial contamination with qualitative bioluminescence imaging and Gram-positive staining and with quantitative bacterial count. Bone changes in terms of resorption and osteomyelitis were quantitatively analyzed through micro-CT (bone mineral density) and semiquantitatively through histologic scoring systems.

Results Six weeks after implantation, we found only a mild decrease in bacterial count in coated versus uncoated implants (Ti versus controls: mean difference [MD], -3.705; 95% confidence interval [CI], -4.416 to -2.994; $p < 0.001$; TiVE versus controls: MD, -3.063; 95% CI, -3.672 to -2.454; $p < 0.001$), whereas micro-CT analysis showed a higher bone mineral density at the knee and femoral metaphysis in the vitamin E-treated group compared with uncoated implants (knee joint: MD, -11.88; 95% CI, -16.100 to -7.664; $p < 0.001$ and femoral metaphysis: MD, -19.87; 95% CI, -28.82 to -10.93; $p < 0.001$). We found decreased osteonecrosis (difference between medians, 1.5; 95% CI, 1-2; $p < 0.002$) in the infected group receiving the vitamin E-coated nails compared with the uncoated nails.

Conclusions These preliminary findings indicate that vitamin E phosphate implant coatings can exert a protective effect on bone deposition in a highly contaminated animal model of implant-related infection.

Clinical Relevance The use of vitamin E coatings may open new perspectives for developing coatings that can limit septic loosening of infected implants with bacterial contamination. However, a deeper insight into the mechanism of action and the local release of vitamin E as a coating for orthopaedic implants is required to be used in clinics in the near future. Although this study cannot support the antimicrobial properties of vitamin E, promising results were obtained for bone-implant osseointegration. These preliminary results will require further in vivo investigations to optimize the host response in the presence of antibiotic prophylaxis.

Introduction

Periprosthetic joint infections (PJIs) represent a severe complication and a clinical burden after total arthroplasty, occurring in some series in as many as 3% of primary knee and hip implant procedures [45] and up to 15.4% of hip and 25% of knee implant revisions [19]. The PJI risk may be as high as 36% when associated with the use of megaprostheses for large bone removal or tumor surgery [17]. These infections are biofilm-related and are mainly caused by *Staphylococcus* species [29, 43]. To reduce the risk of PJI and implant-related infections, several antibacterial coatings have been studied during the last decade [15, 38]. Although research has focused on the development of effective antimicrobial surfaces to prevent bacterial adhesion and proliferation on prosthetic implants, no effective strategy has been developed to reduce the impact of bacteria on the surrounding tissues, including inflammation and bone loss, which are the main results of bacterial colonization of biomaterials. This is particularly important in orthopaedics, in which maintaining functional activity of resident cells is mandatory for good osseointegration of the prosthesis [8].

Recent studies have investigated the immunomodulatory and antibacterial properties of vitamin E (α-tocopherol) and of its acetate and phosphate esters against Gram-positive and Gram-negative bacteria [2, 6, 7]. Our group found differences in antimicrobial activity among various forms of vitamin E, in which the water-soluble phosphate ester form showed a direct in vitro antimicrobial effect on antiadhesion and antibiofilm activities [6]. These findings were similar to previous investigations that reported how vitamin E may reduce bacterial adhesion as a result of its antioxidant property through inhibition of bacterial exopolymer-producing enzymes and through the modulation of the immune function, thus reducing the bacterial colonization [3, 4, 14, 20]. Moreover, the study by Bidossi et al. [6] demonstrated in vitro that the vitamin E phosphate form was consistently absorbed into the titanium surface without diffusing into the surrounding environment. Other studies focused on both the immunomodulatory and anabolic capabilities of vitamin E [12, 27, 33]; in human subjects and animal models, high doses of vitamin E exhibited antiinflammatory effects by decreasing C-reactive protein and inhibiting the release of proinflammatory cytokines [13, 41]. Because vitamin E also inhibited cyclooxygenase-2 activity, it was thought to exert antiinflammatory and anticarcinogenic activities [18]. This was demonstrated by Yang and colleagues [46], who found that vitamin E lowered the colon inflammation index and reduced the number of colon adenomas in mice. More recently, various vitamin E formulations have been shown to suppress bone resorption cytokines [32].

Based on these findings, we investigated whether a vitamin E phosphate coating on titanium implants may reduce (1) bacterial colonization of prosthetic implants and (2) bone resorption and osteomyelitis in a rat model of *Staphylococcus aureus*-induced implant-related infection.

Materials and Methods

Twenty 12-week-old Wistar male rats (Envigo RMS Srl, San Pietro al Natisone, Udine, Italy) were randomly

assigned to the control (Control) group, which were injected with 5 μL of phosphate-buffered saline (PBS; n = 8) or to the infected group (Xen40; n = 12), which were injected with 5 μL of a PBS suspension containing 3 x 10^4 colony-forming units (CFU) of the bioluminescent strain *S aureus* UAMS-1Xen40 (No. 119244; Perkin Elmer Inc, Waltham, MA, USA). The control group was included to assess infection development in the Xen40 group as well as the host and tissue responses toward the vitamin E-coated implants. All animals bilaterally received smooth titanium Kirschner wires that were coated with vitamin E (TiVE) or left uncoated (Ti) within the femoral canal to generate an internal control, as described in Shiels et al. [39].

To assess animal welfare and the development of the infections, we monitored both control and Xen40-infected rats for body weight and neutrophil count compared with the baseline at Day 0. The bacterial colonization of the Xen40 group was evaluated through qualitative analyses (bioluminescence imaging and Gram-positive staining) and quantitative microbiologic tests (Day 42) by comparing Ti- and TiVE-implanted limbs. Quantitative micro-CT and semiquantitative histologic analyses were performed to evaluate bone resorption and osteomyelitis between groups (Table 1).

The Mario Negri Institute for Pharmacological Research (IRFMN) Animal Care and Use Committee approved the entire study (Permit No. 1079/2016-PR). The animals were housed at the institute's animal care facilities according to international standards. The IRFMN adheres to the principles set out in the following laws, regulations, and policies governing the care and use of laboratory animals: D.lgs 26/2014; Authorization n.19/2008-A issued March 6, 2008, by the Ministry of Health. The animals were regularly checked by a certified veterinarian responsible for animal welfare. All surgeries were performed under general anesthesia, and all efforts were made to minimize suffering according to the experimental design. In this study, the use of laboratory animals was necessary to assess the host response and the complex mechanisms involved in the case of an implant-related infection that is not possible to test in vitro. The choice of the rat as the model for this study follows the principles of the lowest neural development with appropriate limb dimensions for the implant technique and resembling human responses.

Preparation of S aureus Xen40 Inocula

We streaked bacteria onto tryptic soy agar plates (BioMérieux, Marcy-l'Étoile, France) and incubated them overnight at 37° C under aerobic conditions. Then, the culture was diluted with PBS to a 0.5 McFarland standard to a final bacterial load of 3 x 10^4 CFU/5 μL, confirmed by viable plate count as we previously described [24, 26].

Preparation of Titanium Implants and Vitamin E-based Compound

Titanium Kirschner wires (Ti-6Al-4V, 1.25 mm in diameter) were coated with the vitamin E-based compound (TiVE) or left uncoated (Ti).

Stock solutions of α-tocopherol phosphate (Sigma-Aldrich, St Louis, MO, USA) were prepared by dissolving α-tocopherol phosphate into sterile dH_2O at a concentration of 20% (w/v) and kept at 4° C until use.

Table 1. Number of animals per group and investigation

Analyses	Uninfected control group	Xen40-infected group (Xen40)
Total animals (N) and samples (n)	N = 8	N = 12
	Ti (n = 8); TiVE (n = 8)	Ti (n = 12); TiVE (n = 12)
Lost animals (N) and samples (n)	N = 2	N = 3
	Ti (n = 2); TiVE (n = 2)	Ti (n = 3); TiVE (n = 3)
Body weight (weekly)	N = 6	N = 9
Blood tests (Day 42)	N = 6	N = 9
Bioluminescence (Days 0, 3, 42)	none	N = 9
		Ti (n = 9); TiVE (n = 9)
Micro-CT (Day 42)	N = 6	N = 9
	Ti (n = 6); TiVE (n = 6)	Ti (n = 9); TiVE (n = 9)
Microbiologic test (Day 42)	N = 4	N = 5
	Ti (n = 4); TiVE (n = 4)	Ti (n = 5); TiVE (n = 5)
Histology (Day 42)	N = 2	N = 4
	Ti (n = 2); TiVE (n = 2)	Ti (n = 4); TiVE (n = 4)

Xen40 = *Staphylococcus aureus* bioluminescent strain; Ti = titanium implants; TiVE = titanium implants coated with vitamin E.

To obtain a compound with a viscous, antisliding, and hydrophobic consistency for the Kirschner wire coating, the stock solution of α-tocopherol phosphate was dissolved into sterile glycerol (VWR International, Milan, Italy) to obtain a final concentration of vitamin E equal to 5% weight/volume (w/v), as reported by Bidossi et al. [6]. We chose glycerol because it is a nontoxic polyol that is widely used as a solvent in several pharmaceutical formulations [28] and has good biocompatibility [1, 9, 42]. Before implantation, we manually coated the Kirschner wires by immersing the nail directly in the α-tocopherol phosphate. Specifically, 5 mg/cm^2 vitamin E solution formed a thin, viscous lining of approximately 2 mm on the surface of Kirschner wires that were immediately implanted within the femoral canals.

Surgical Procedures

Twenty Wistar rats (male, 8 weeks old, mean body weight, 334.6 ± 9.8 g) were maintained under specific pathogen-free conditions. Under general anesthesia induced with isoflurane (3%; Isoflurane Vet, Merial; Boehringer Ingelheim, Ingelheim, Germany), maintained with an intraperitoneal injection of ketamine hydrochloride (80 mg/kg; Imalgene, Merial; Boehringer Ingelheim) and medetomidine hydrochloride (1 mg/kg; Domitor; Pfizer Italia Srl, Milan, Italy), an incision was made over the knee and a medial parapatellar arthrotomy was created to expose the femoral intercondylar notch. Using 22- and 18-gauge needles, we progressively reamed the medullary canal and then inoculated it with 5 μL of PBS (control group) or with 3 x 10^4 CFU/5 μL of *S aureus* Xen40 (Xen40 group) suspended in PBS by means of a micropipette. We randomly inserted coated or uncoated Kirschner wires into the femoral medullary canal. The correct placement of the Kirschner wires was assessed by fluoroscopic examination (Fig. 1). All animals were treated with carprofen (5 mg/kg; Rimadyl; Pfizer Italia Srl, Milan, Italy). Pain was controlled with buprenorphine (0.1 mg/kg subcutaneous; Temgesic; Schering-Plough SpA, Segrate, Milan, Italy). No local or systemic antibiotics were administered to avoid masking the antimicrobial effects of the tested coating. Rats were caged paired until the end of the study. We monitored the rats daily for general status, clinical signs of infection, lameness, swelling, exudate, hematoma, and pain. On Day 42, the rats were euthanized by CO_2 inhalation and bones/tissues were aseptically retrieved.

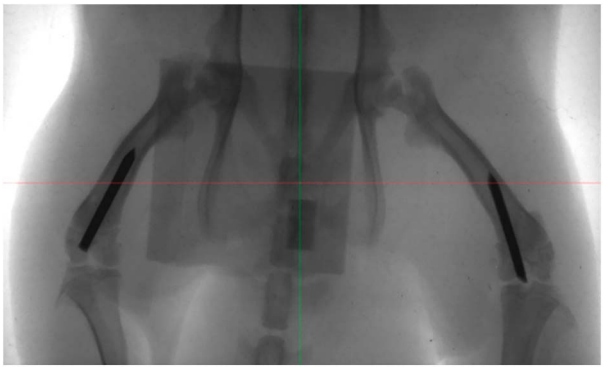

Fig. 1 The fluoroscopic examination that assesses the correct position of Kirschner wires in the femurs is shown.

Body Weight and Blood Analyses

We measured body weight before surgery and weekly thereafter. Under general anesthesia, we collected blood samples from the tail vein to determine the peripheral neutrophil count by using an automatic cell counter (Sysmex XT-1800i, Dasit; Cornaredo, Milan, Italy) [24, 26]. Body weight measurements are reported as raw data and normalized to the basal values at Day 0 (Control, n = 6; Xen40, n = 9); the neutrophil count is reported as raw data at Day 42 (Control, n = 6; Xen40, n = 9).

In Vivo Bioluminescence Imaging

On Days 0, 3, and 42, we used bioluminescence imaging to monitor infection progression in the presence of bioluminescent *S aureus* in the Xen40 group (n = 9). Under general anesthesia, we scanned the rats with optical imaging (eXplore Optix MX2; Advanced Research Technologies Inc, Saint-Laurent, Canada) using a photomultiplier tube to detect optical photos of 450 nm to 900 nm in wavelength. Image acquisition was performed using a raster scan model with a resolution of 1.5 mm by analyzing a fixed region of interest centered on the operated limb. Images were analyzed using Optix OptiView software (Version 2.01; Advanced Research Technologies Inc) and the bacterial burden was expressed as photon counts. Data were normalized to the brightness of the signal on Day 0 and presented on a color scale overlaid on grayscale photographs of the rats.

Microbiologic Analyses

On Day 42, microbiologic tests were carried out to quantify viable bacteria within the explanted samples. Specifically, after euthanizing animals, samples consisting of the entire knee, the Kirschner wire implant, and the periimplant soft tissues were collected from each group (Control, n = 4; Xen40, n = 5), then weighed and treated with dithiothreitol (DTT) to retrieve viable bacteria within the biofilm instead

of by conventional sonication [24, 26]. A solution of 0.1% w/v DTT in PBS (Sigma-Aldrich) was added to the samples and stirred for 15 minutes at room temperature to detach bacteria from the biofilm. After centrifuging, bacterial pellets were suspended in 1 mL of the DTT eluate. Then, 100 μL was plated onto blood agar plates and inoculated into the brain heart infusion broth, according to the clinical laboratory testing and in vitro diagnostic test systems by the International Organization for Standardization (ISO) Technical Committee 212 (ISO/TC 212). Plates were incubated for 48 hours at 37° C, while broth cultures were incubated for 15 days. Then, 10 μL of each turbid broth culture was plated onto blood agar plates and incubated for 24 hours at 37° C. Formed colonies were Gram-stained and assessed for catalase, coagulase, and for growth on Mannitol salt agar. Mannitol-positive, coagulase-positive, golden yellow, smooth colonies were counted. The log (CFU)/g explant was determined by dividing the log CFU number by the initial total weight of the sample. Nondetectable values (nd) ≤ logarithm of odds (LOD) was set at 0.18 log (CFU)/g explant.

Micro-CT Imaging and Data Analysis

To evaluate bone reaction in terms of bone resorption and osteomyelitis, micro-CT analysis was performed on all rats with a scanner (Explore Locus; GE Healthcare, Little Chalfont, Buckinghamshire, UK) using 80-kV voltage, 400-μA current with 400-msec exposure time per projection and 400 projections over 360°, a total scan time of 10 minutes, and an isotropic resolution of 93 μm. We analyzed the three-dimensional reconstructed images with MicroView version 2.1.2 software (GE Healthcare). After scan calibration, we created two box volumes of interest: the first sized 440 mm^3 (X: 15; Y: 15; Z: 20) between the femoral and tibial metaphysis, including the knee and the femoral and tibial epiphysis; and the second sized 200 mm^3 (X: 8; Y: 8; Z: 8) including the femoral metaphysis. The bone mineral density (BMD, mg/cc) within these two volumes of interest was quantitatively measured and reported as the percentage of relative decrease in the Control group. Histogram-based isosurface renderings were performed on the knee and femoral metaphysis to obtain a qualitative assessment of the bone and periimplant tissues to better appreciate the gross changes.

Histologic Analyses

Histologic analyses were carried out to assess the tissue morphology with particular attention toward signs of inflammation, bone necrosis, and osteomyelitis as well as to verify the presence or absence of bacteria in the samples. After euthanasia, excised entire knees (Control, n = 2; Xen40, n = 4) were fixed in 10% formalin for 48 hours, then decalcified in disodium EDTA/acid buffer (Osteodec; Bio-Optica, Milan, Italy) under agitation for 5 days. The specimens were dehydrated, embedded in paraffin, and cut into 3.5-μm sections. Tissue morphology was evaluated by hematoxylin and eosin staining, and the presence or absence of bacteria was confirmed by Gram staining as a qualitative analysis to support the microbiologic tests. Photomicrographs were captured using a light microscope and a camera (Olympus IX71 and Olympus XC10). Three blinded observers (ABL, MB, CLR) evaluated signs of femoral metaphysis osteomyelitis according to the modified Petty's score, as we previously described [25, 26]. Specifically, this semiquantitative score from 0 to 3 indicates: 0 = absence of bone reaction and inflammatory cells; 1 = layered periosteum, presence of occasional polymorph nucleated leukocytes; 2 = sunburst periosteum, granulation tissue, fragmented polymorph nucleated leukocytes and osteoclasts, several microabscesses in the medullary canal; 3 = florid periosteum, subperiosteal, endosteal and intracortical resorption, and several micro- and great abscesses with diffuse polymorph nucleated leukocytes within the medullary canal.

Signs of osteomyelitis were also assessed at the knee level according to the Histopathological Osteomyelitis Evaluation Score (HOES) reported by Tiemann et al. [44].

The HOES score assesses patterns of acute and chronic osteomyelitis specifically related to infections of both soft tissue and osseous fractions. In particular, the HOES score distinguishes osteomyelitis as acute, chronically active, chronic, or calmed ranging from 0 to 3, and it is based on the evaluation of these main osseous changes (osteonecrosis and bone neogenesis), soft tissue changes (necrosis), and inflammatory infiltration.

Statistical Analysis

Data were analyzed for normal distribution by means of Kolmogorov-Smirnov test. Body weight comparisons between groups and time points were analyzed using two-way analysis of variance (ANOVA) (GraphPad Prism v6.00; GraphPad Software, Inc, La Jolla, CA, USA) coupled with Bonferroni's post hoc test and reported as mean ± SD. Microbiologic data were analyzed using one-way ANOVA coupled with Tukey's post hoc and reported as mean ± SD. Neutrophil counts and histologic scores were analyzed using the two-tailed Mann-Whitney test and reported as median ± difference between medians. Micro-CT quantitative data were analyzed with unpaired t-test and reported as mean ± SD. The interrater reliability of the examiners' scores was calculated using the intraclass

correlation coefficient (ICC). The obtained interrater reliability of blind scoring was rated excellent (ICC = 0.930). Values of $p < 0.050$ were considered significant. The sample size provided 80% power to detect a difference for the presence or absence of osteolysis of the tested coatings using a two-sided t-test with $\alpha = 0.050$ (G*Power 3.1, Düsseldorf, Germany).

Results

Clinical Examination

Approximately 4 to 6 hours after surgery, five animals in the Control (n = 2) and Xen40 groups (n = 3) were euthanized as a result of surgical complications consisting of swelling and congestion of both the operated limbs associated with extensive caudal necrosis. Histologically, these complications were caused by deep venous fat embolism secondary to the lower extremity surgery (data not shown), described by Mueller et al. [30] as a rare occurrence after intramedullary nailing. None of the remaining animals died during the followup period, although we observed a more aggressive attitude in some animals. The analyses were thus performed on the remaining samples.

Body weight decreased in all rats 10 days after surgery with a larger decrease in the Xen40 group compared with the control group (Fig. 2A; see Table 1, Supplemental Digital Content). After Day 10, relative body weight in the control group increased and returned to a normal growth curve (Fig. 2B). Starting on Day 35, body weight began to increase in the Xen40 group but remained lower overall compared with the control group (see Table 2, Supplemental Digital Content).

On Day 42, blood tests indicated a neutrophil count increase in the Xen40 group compared with the control group (difference between medians, -0.855; 95% confidence interval [CI], -1.450 to 0.030; p = 0.042).

Effects of Vitamin E Coating on Bacterial Colonization

On Days 0 and 3, bioluminescence images qualitatively showed the presence of metabolically active bioluminescent bacteria at the injection site. By Day 42, the bioluminescence signal diminished to undetectable levels (Fig. 3). However, in most cases, a different intensity of bioluminescence signal was found in the infected limbs, despite having been inoculated with the same bacterial load (3×10^4 CFU) (Fig. 3).

We observed no bacteria growth in the control group (Ti, n = 4; TiVE, n = 4; nd ≤ LOD set at 0.18 log [CFU]/g explant). In the Xen40 group, bacterial counts were 3.8 ± 0.4 and 3.2 ± 0.5 log (CFU)/g explant, respectively, for the Ti (n = 5) and TiVE (n = 5) groups with a difference with the control group that resulted as nondetectable values (Ti versus controls: mean difference [MD], -3.705; 95% CI, -4.416 to -2.994; $p < 0.001$; TiVE versus controls: MD, -3.063; 95% CI, -3.672 to -2.454; $p < 0.001$). There was no difference between the Xen40 groups treated with Ti or TiVE with the numbers available (MD, 0.642; 95% CI, -0.092 to 1.377; p = 0.088).

Effects of Vitamin E Coating on Bone Resorption and Osteomyelitis

Micro-CT analysis gave both qualitative and quantitative results. Specifically, micro-CT qualitatively showed complete preservation of the normal knee and femoral metaphysis in the control group, regardless of the coating type (Ti, n = 6; TiVE, n = 6); thus, data obtained from these animals were grouped. The quantitative

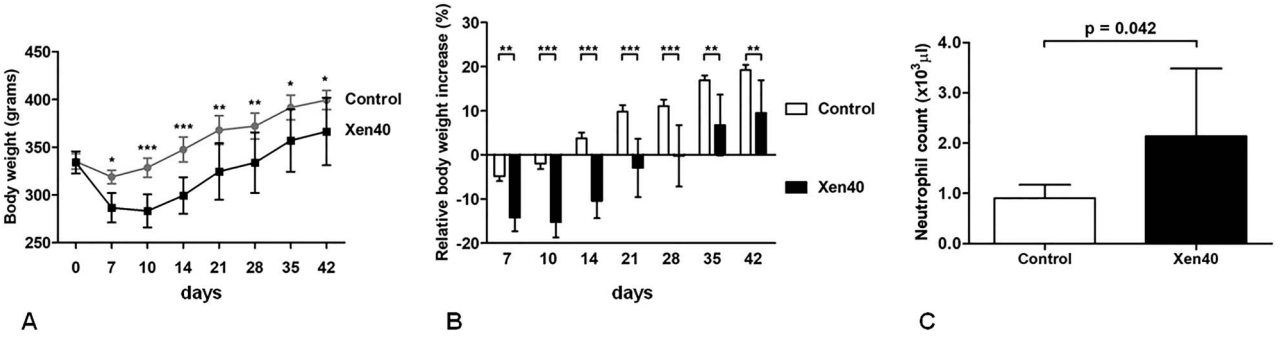

Fig. 2 A-C Clinical data report the raw data of body weight (grams) over time as the mean ± SD (**A**) as well as the percentage of relative body weight increase normalized to the baseline at Day 0 as the mean ± SD (**B**). The blood neutrophil count on Day 42 is reported in the histogram as the median with 95% CI (**C**). Data are referred to the Control group (Control, n = 6) and to the infected group (Xen40, n = 9). *$p < 0.05$, **$p < 0.01$, ***$p < 0.001$.

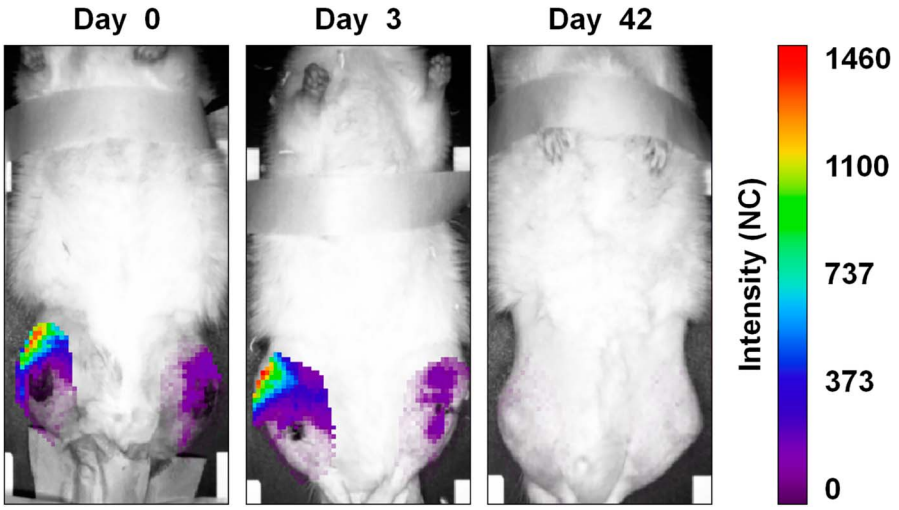

Fig. 3 The figure depicts a representative panel of bioluminescence imaging analysis in the infected Xen40 group. Rats receiving the femoral canal injection of 3 x 10^4 CFU *S aureus* Xen40 showed the signal of the bioluminescent bacteria with differences between the injected limbs on Days 0 and 3. On Day 42, no bioluminescent signal was detected. Data at Days 3 and 42 are reported as normalized to the bioluminescence signal on Day 0. The intensity of the bioluminescence signal is measured as normalized photon counts (NC).

assessment of BMD showed a large BMD decrease both in Ti (n = 9) and TiVE (n = 9) in the Xen40 group (Fig. 4). However, the analysis of the whole knee showed a greater BMD with TiVE compared with Ti (MD, -11.88; 95% CI, -16.100 to -7.664; $p < 0.001$). At the femoral metaphysis level, where the coating can be expected to exert maximum implant protection, we measured a BMD reduction in Ti implants compared with TiVE implants (MD, -19.87; 95% CI, -28.82 to -10.93; $p < 0.001$), in which BMD was unchanged. These results were consistent with thinned bone and periarticular tissue fragments suggestive of an active infection destroying the articular surfaces and the subchondral bone in Ti knees in the Xen40 group (Fig. 5). Similarly, multifocal zones of osteolysis, cortical bone enlargement, and severe subperiosteal reaction were also found in the femoral metaphysis of these rats. We saw fewer signs of infection in the Xen40 group treated with TiVE, and we found only a subperiosteal reaction at the femoral metaphysis. We identified more bone deposition in the TiVE group compared with Ti, as supported by the higher BMD detected in this group. The isosurface reconstruction on Day 42 (Fig. 6) showed that the control group presents a smooth bone surface both in the knee and femoral metaphysis. The Xen40 group treated with Ti shows an appreciable rough bone texture

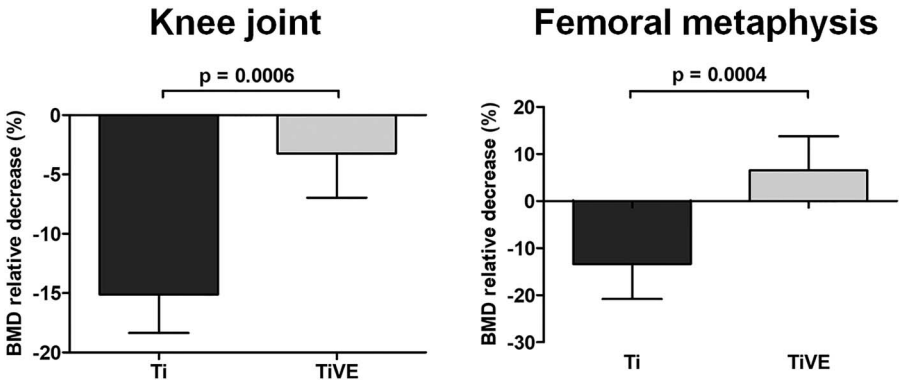

Fig. 4 The figure reports the micro-CT-based quantitative analysis of the entire knee and metaphysis of femurs. BMD is reported as the percentage of relative decrease in the Xen40 group with respect to the control group on Day 42 and data are expressed as mean ± SD. Data are referred to the Xen40 group (Ti, n = 9; TiVE, n = 9); $^{**}p < 0.01$, $^{***}p < 0.001$.

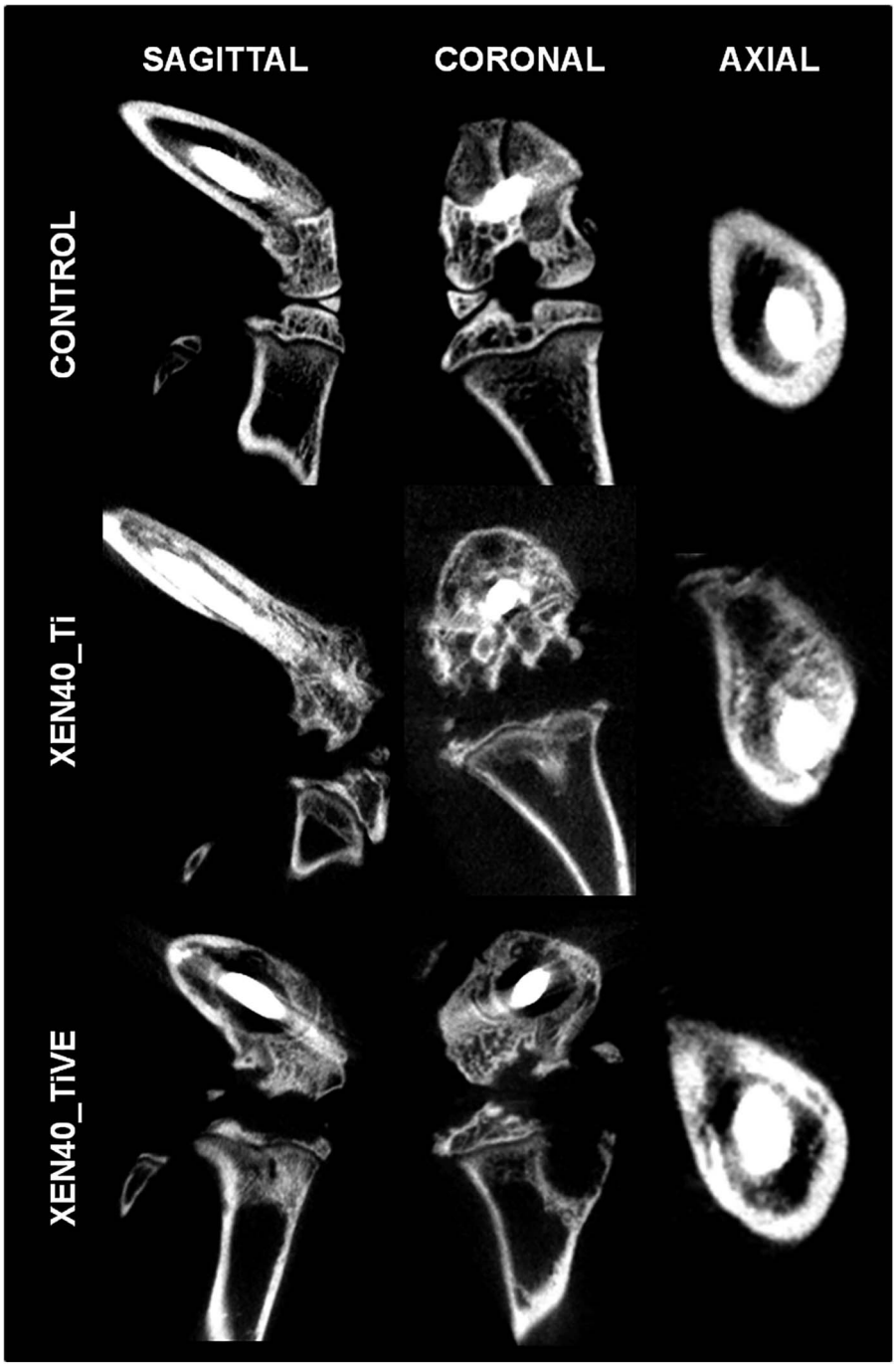

Fig. 5 The representative panel shows qualitative micro-CT images of Day 42 samples in the uninfected control (Control) and infected groups (Xen40) implanted with Ti and TiVE. The sagittal and coronal planes include the entire knee; the axial plane reports information of the femoral metaphysis. The control group presents complete integrity of the bone structure both in the knee and femoral metaphysis. Severe signs of osteomyelitis are represented by a wide or mild bone rarefaction in the Xen40 group receiving Ti or TIVE treatment, respectively.

as a sign of osteomyelitis. The Xen40 group treated with TiVE shows a denser bone surface compared with Ti as a sign of bone deposition.

Qualitative histology (Fig. 7) indicated that physiological findings were independent of the coating in the control group (Ti, n = 2; TiVE, n = 2) with an intact

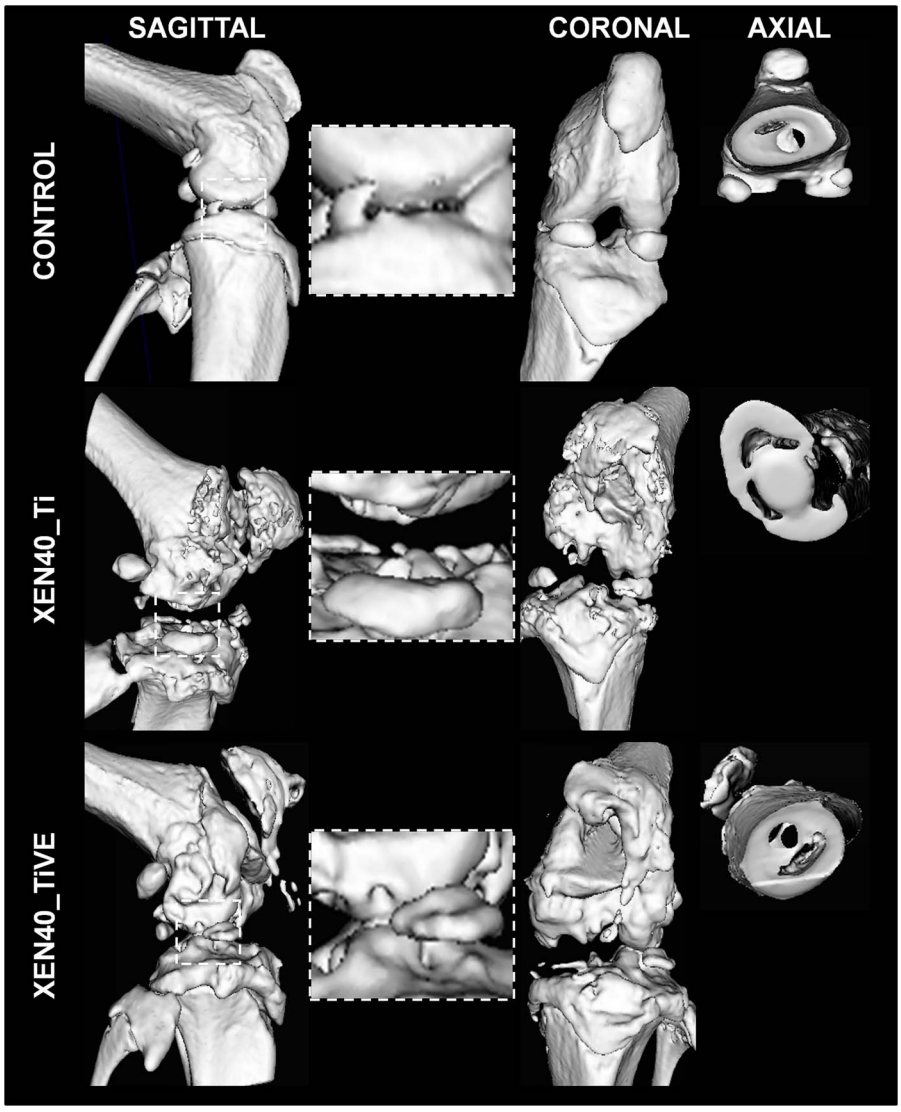

Fig. 6 The representative panel shows Day 42 three-dimensional isosurface reconstructions. Images are presented for the uninfected control (Control) and infected group (Xen40) implanted with Ti and TiVE. The sagittal and coronal planes include the entire knee, whereas the axial plane includes the femoral metaphysis. The control group presents a smooth bone surface both in the knee and femoral metaphysis. The Xen40 group treated with Ti shows an appreciable rough bone texture as a sign of osteomyelitis. The Xen40 group treated with TiVE shows a denser bone surface compared with Ti as a sign of bone deposition.

appearance of the knee, the cortical bone, and the periosteum of the femoral metaphysis. We found no signs of inflammatory infiltrates or granulation tissue in the control group. The Xen40 samples (Ti, n = 4; TiVE, n = 4) showed irregular contours of the knee in which several micro- and macroabscesses were present in the periarticular soft tissues of Ti-implanted joints. In Ti-implanted joints, we detected abscesses within the medullary space at the femoral metaphysis. In the Xen40 group, clear cortical bone enlargement and two to three laminated periosteal reactions were found in the metaphysis.

We mainly found signs of osteomyelitis such as intramedullary abscesses, necrotic bone sequestra, and osteoclasts (Fig. 8A-B) in the Xen40 group implanted with Ti. Soft tissue abscesses and plasma cells were found in the joint space of Ti (Fig. 8C). The formation of granulation tissue within the medullary trabeculae and several osteoblasts were found in all samples of the Xen40 group (Fig. 8D) as well as enhancement of the

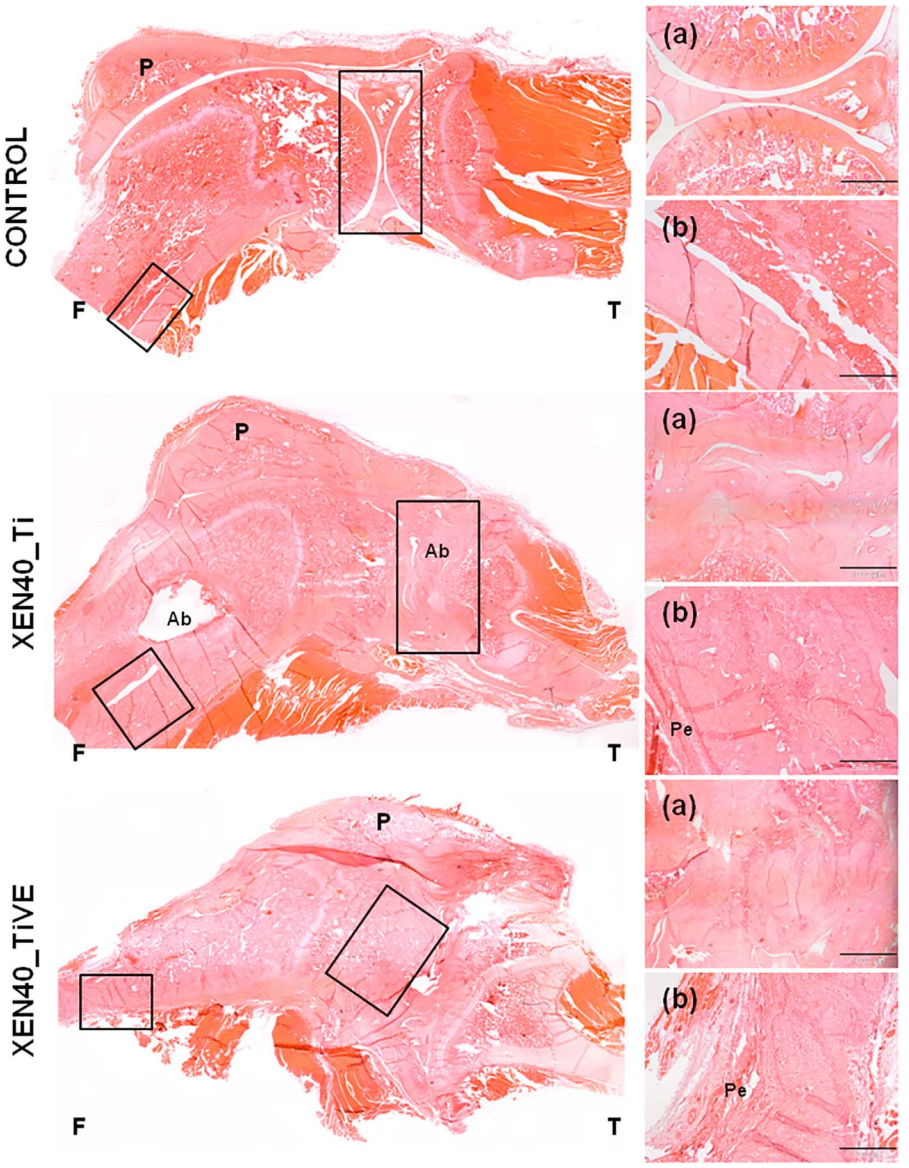

Fig. 7 The representative panel shows the histologic analysis (hematoxylin and eosin) of the control (Control) and the infected groups (Xen40) implanted with Ti and TiVE Kirschner wires. The control group shows an intact appearance of bone and articular cartilage of the knee as well as well-preserved cortical bone in terms of structure and thickness of the femoral metaphysis. The Xen40 group treated with Ti shows irregular contours of the joint with the presence of abscesses; abscesses are also present at the level of the femoral metaphysis characterized by enlargement of the medullary space together with a periosteal reaction. Despite the irregular contour of the joint, the Xen40 group treated with TiVE does not show any presence of abscesses; a similar periosteal reaction of Ti is depicted at the femoral metaphysis of TiVE. F = femur; T = tibia; P = patella; Ab = abscesses; Pe = periosteum. In the small boxes are depicted: (**a**) articular joint, original magnification, x 2, scale bar 1000 μm; (**b**) metaphyseal cortex, original magnification, x 4, scale bar 500 μm.

vascular invasion within bone and soft tissues (Fig. 8E-F). As signs of bone neogenesis, a reactive bone network represented by the presence of new woven bone along with lamellar bone was found in the Xen40 group implanted with TiVE-coated implants (Fig. 8G). In the Xen40 group treated both with Ti or TiVE, the presence of cocci within abscesses was detected by the Gram-positive staining (Fig. 8H).

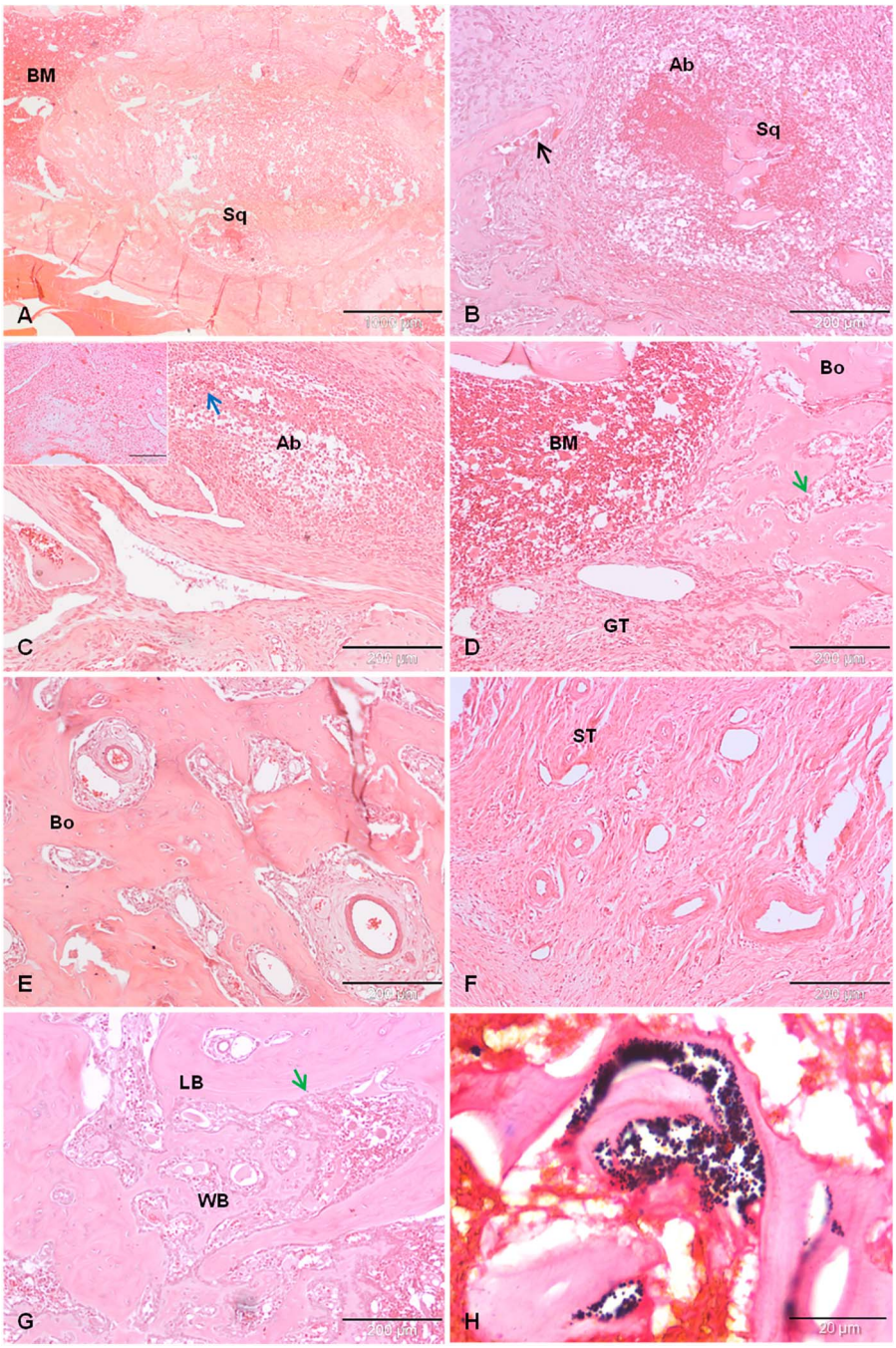

Fig. 8 A-H This panel reports the following histopathologic details: (**A**) endomedullary abscess with necrotic bone sequestrum (Sq); (**B**) endomedullary abscess (Ab) with necrotic bone sequestrum (Sq) and osteoclasts (black arrow); (**C**) soft tissue abscess, infected tissue (blue arrow) and plasma cells (small box); (**D**) granulation tissue (GT) and several osteoblasts (green arrow) within the bone marrow (BM) and bone trabeculae (Bo); (**E**) hypervascularization within the bone tissue (Bo); (**F**) hypervascularization of the soft tissues (ST); (**G**) bone neogenesis with formation of woven bone (WB) alongside lamellar bone (LB) and osteoblasts (green arrow); and (**H**) Gram-positive staining of *S aureus* Xen40. Panel (**A**) original magnification, x 2, scale bar 1000 µm; Panels (**B-G**) original magnification, x 10, scale bar 200 µm; Panel (**H**) original magnification, x 100, scales bar 20 µm.

Overall, the semiquantitative Petty's scale for the femoral metaphysis showed a higher score in the Xen40 group compared with the control group (Ti versus controls: difference between medians, -2; 95% CI, -2 to -0.5; $p < 0.001$ and TiVE versus controls: difference between medians, -2; 95% CI, -2 to -1; $p < 0.001$), but no differences were found between Ti and TiVE implants (difference between medians, 0.0; 95% CI, -1 to -1; $p = 0.860$) (Fig. 9A).

The HOES score measured that osteonecrosis was higher in the Xen40 group compared with the control group (Ti versus controls: difference between medians, -3; 95% CI, -3 to -2.8; $p < 0.001$ and TiVE versus controls: difference between medians, -1.5; 95% CI, -1.8 to -1; $p < 0.001$), but osteonecrosis was lower in the TiVE group compared with the Ti group (difference between medians, 1.5; 95% CI, 1-2; $p < 0.002$) (Fig. 9B). The inflammatory pattern of HOES score measured a difference between the Xen40 group and controls (Ti versus controls: difference between medians, -3; 95% CI, -3 to -2.5; $p < 0.001$ and TiVE versus controls: difference between medians, -3; 95% CI, -3 to -3; $p < 0.001$), whereas no differences were measured between Ti and TiVE (difference between medians, 0.0; 95% CI, 0.0-0.0; $p = 0.203$) (Fig. 9C). Finally, the bone neogenesis by HOES score measured a greater trend both in Ti- and TiVE-treated Xen40 groups compared with the controls (Ti versus controls: difference between medians, 0.0; 95% CI, -0.80 to -0; $p = 0.002$ and TiVE versus controls: difference between medians, -0.5; 95% CI, -1 to -0.0; $p < 0.001$); no differences were found between Ti and TiVE in the Xen40 group (difference between medians, -0.5; 95% CI, -0.5 to 0.0; $p = 0.675$) (Fig. 9D).

Discussion

To reduce the risk of progressive bone loss and implant loosening in the case of PJIs and osteomyelitis, several antibacterial coatings have been studied during the last decade [15, 29, 38, 43]. In vitro antiadhesive and antibacterial properties and in vivo antiinflammatory effects protecting against bone loss of various formulations of vitamin E have been demonstrated in animal models. However, to the best of our knowledge, no in vivo studies have demonstrated the synergistic activity of vitamin E in the form of a coating in preventing the bacterial adhesion to orthopaedic implants, thus supporting bone-implant integration. To our knowledge, the present study shows for the first time that a vitamin E-based coating can reduce the detrimental effects of bacterial colonization of a prosthetic implant on bone tissue. We evaluated the impact of this coating on bone response in the presence of osteomyelitis

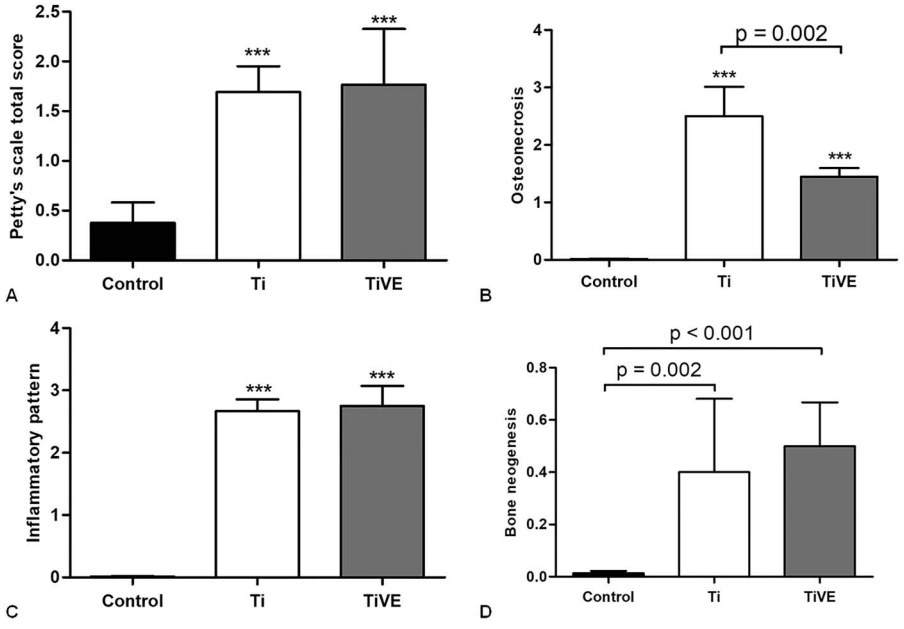

Fig. 9 A-D Petty's scale is reported as the total score comparing the Control group (Control) with the infected group (Xen40) differently treated with Ti or TiVE on Day 42 (**A**). The HOES scale measurements of the femoral metaphysis and joint are reported separated for the three main features analyzed such as osteonecrosis (**B**), inflammatory pattern (**C**), and bone neogenesis (**D**) on Day 42. Data are reported as median with 95% CI. $^{***}p < 0.001$ with respect to the Control (Control) group.

at the articular joint and metaphysis in a rat model of highly contaminated *S aureus* implant-related infection.

This study had limitations. This study used a very simple rat model and a small sample size in terms of number of animals used. However, the good reproducibility of our infection model–demonstrated by comparing with a control group and the choice to implant each animal bilaterally in the femurs–allowed us to answer the questions of this study. The sample size was also limited by the mortality of some rats resulting from unexpected surgical complications. This suggests that bilateral implant placement can be at higher risk compared with a monolateral approach. Another limitation of this study is that the high bacterial load model may not necessarily reflect the clinical conditions. However, although the high bacterial load (3×10^4 CFU Xen40) used and the absence of systemic or local antibiotic prophylaxis do not exactly mimic clinical conditions in elective surgery, we considered that smaller loads could fail to develop a high number of infected animals as a result of high-level rat immunity against bacteria, as demonstrated by Lovati et al. and Shimazaki et al. [23, 26, 40]. Hence, the high bacterial load used in rats was necessary to have good reproducibility in the model. Moreover, other microorganisms than *S aureus* and their toxic effects should be investigated because their consequences on bone may not be the same. In our experimental condition, we demonstrated the positive activity on bone of the vitamin E coating in bone damage (osteomyelitis) caused by a *S aureus* strain. The coating supported bone deposition in the presence of a high virulence pathogen, thus supposing that vitamin E coating can work also in the presence of lower virulent strains such as *Staphylococcus epidermidis*. Also, the mechanisms of action of vitamin E phosphate, its pharmacokinetics, and degradation were not elucidated in the present study and must be further assessed.

Bioluminescence imaging analysis revealed in all groups the presence of metabolically active bacteria from Day 0 to Day 3 followed by a bioluminescence signal decrease suggesting a reduction of the metabolic rate of bacteria embedded within the biofilm as a result of a quiescent state. This finding is also in line with other studies using bioluminescent bacteria for similar purposes in mice [21, 35]. However, the differences detected in the bioluminescence signal in both limbs injected with the same bacterial load may represent a limitation of this qualitative analysis. Thus, to confirm the presence of bacteria, we performed microbiologic tests on the explants. Microbiologic findings (1) could not confirm the expected vitamin E coating's antimicrobial activity based on its antiadhesive properties demonstrated in vitro [6, 20, 22], probably as a result of the high bacterial inoculum and the absence of an antibiotic prophylaxis used in the present in vivo study. The present study better supports the promising potential of vitamin E in diminishing bone signs of infection by enhancing the local bone response in the presence of a contaminated implant. Indeed, (2) the present model demonstrated that the vitamin E phosphate coating increased new bone deposition hypothesizing stimulation of bone precursor cells and osteoblasts to depose newly bone matrix also in the case of bacterial-induced chronic osteomyelitis. In fact, TiVE demonstrated enhanced new bone deposition, even in the presence of a chronic bacterial infection, when compared with Ti. Similarly, osteonecrosis was clearly reduced in TiVE compared with Ti. Concerning the mechanism of action, we speculate that the protective effect of vitamin E phosphate on bone changes with infection is related to the antioxidant properties of vitamin E. Indeed, our findings can be in line with the ability of vitamin E-loaded polyethylene to protect against osteolysis associated with wear debris in arthroplasty [5, 11, 34]. The beneficial effect on bone deposition could probably be better executed with local delivery rather than with systemic supplementation. In fact, other reviews have shown that systemic administration of vitamin E supplements may have complex and contradictory effects on bone formation [10, 16, 31], but not clear activity in bone deposition as we obtained by local delivery of vitamin E. No cytotoxic or inflammatory effects of the vitamin E coating were found on bone cells and periarticular tissue effects, thus supporting the good biocompatibility of this coating.

The findings of this preliminary in vivo rat study indicate that the vitamin E phosphate-coated implants can exert a protective effect on bone deposition in a highly contaminated model of implant-related infection. The present study shows that it is possible to distinguish between an antibacterial effect and a protective effect on bone healing and osseointegration in an induced implant-related infection. On the basis of our data, we may not fully anticipate what the clinical applications of this observation will be. However, we may speculate that at least three possible scenarios can be feasible. In the first one, a vitamin E-based protective coating may be designed to simply allow better bone healing and osseointegration in the presence of bacterial contamination reducing implant malfunction resulting from prosthetic loosening [37]. A second possible application concerns the possibility of coupling the protective effect of vitamin E on bone healing with one or more antibiotics, as already done with other antimicrobial delivery systems [36]. A third scenario relates to a long-lasting vitamin E composition that may allow longer term protection in the case of an established infection or in the presence of late contamination of the implant. All of these applications are currently under investigation. The use of vitamin E may thus open new avenues for developing coatings that can limit infection-related loosening of infected implants in bacterial contamination. Future research must investigate the effect of

the vitamin E coating with lower bacterial inocula or in combination with standard antimicrobial prophylaxis. Also, it may be of interest to evaluate the behavior of vitamin E as an antibiotic carrier to eventually control implant-related infection while stimulating bone healing and prosthetic osseointegration.

Acknowledgments We thank the Waldemar LINK GmbH & Co (KG, Germany) for providing the titanium Kirschner wires. We also thank Elinor deLancey Pulcini for assistance in editing the manuscript.

References

1. Aberg J, Henriksson HB, Engqvist H, Palmquist A, Brantsing C, Lindahl A, Thomsen P, Brisby H. Biocompatibility and resorption of a radiopaque premixed calcium phosphate cement. *J Biomed Mater Res A.* 2001;100:1269–1278.
2. Al-Salih DAAK, Aziz FM, Mshimesh BAR, Jehad MT. Antibacterial effects of vitamin E: in vitro study. *J Biotech Res Center.* 2013;7:17–23.
3. Banche G, Bracco P, Allizond V, Bistolfi A, Boffano M, Cimino A, Brach del Prever EM, Cuffini AM. Do crosslinking and vitamin E stabilization influence microbial adhesions on UHMWPE-based biomaterials? *Clin Orthop Relat Res.* 2015;473:974–986.
4. Banche G, Bracco P, Bistolfi A, Allizond V, Boffano M, Costa L, Cimino A, Cuffini AM, Del Prever EM. Vitamin E blended UHMWPE may have the potential to reduce bacterial adhesive ability. *J Orthop Res.* 2011;29:1662–1667.
5. Bichara DA, Malchau E, Sillesen NH, Cakmak S, Nielsen GP, Muratoglu OK. Vitamin E-diffused highly cross-linked UHMWPE particles induce less osteolysis compared to highly cross-linked virgin UHMWPE particles in vivo. *J Arthroplasty.* 2014;29:232–237.
6. Bidossi A, Bortolin M, Toscano M, De Vecchi E, Romanò CL, Mattina R, Drago L. In vitro comparison between α-tocopheryl acetate and α-tocopheryl phosphate against bacteria responsible of prosthetic and joint infections. *PLoS One.* 2017;8:1039.
7. Bou Ghanem EN, Lee JN, Joma BH, Meydani SN, Leong JM, Panda A. The alpha-tocopherol form of vitamin E boosts elastase activity of human PMNs and their ability to kill *Streptococcus pneumoniae. Front Cell Infect Microbiol.* 2017;7:161.
8. Busscher HJ, van der Mei HC, Subbiahdoss G, Jutte PC, van den Dungen JJ, Zaat SA, Schultz MJ, Grainger DW. Biomaterial-associated infection: locating the finish line in the race for the surface. *Sci Transl Med.* 2012;4:153rv10.
9. Cardoso DA, Van den Beucken JJ, Both LL, Bender J, Jansen JA, Leeuwenburgh SC. Gelation and biocompatibility of injectable alginate-calcium phosphate gels for bone regeneration. *J Biomed Mater Res A.* 2014;102:808–817.
10. Chai SC, Wei CI, Brummel-Smith K, Arjmandi BH. The role of vitamin E in reversing bone loss. *Aging Clin Exp Res.* 2008;20: 521–527.
11. Chen W, Bichara DA, Suhardi J, Sheng P, Muratoglu OK. Effects of vitamin E-diffused highly cross-linked UHMWPE particles on inflammation, apoptosis and immune response against *S aureus. Biomaterials.* 2017;143:46–56.
12. De la Fuente M, Hernanz A, Guayerbas N, Victor MV, Arnalich F. Vitamin E ingestion improves several immune functions in elderly men and women. *Free Radic Res.* 2008;42:272–280.
13. Devaraj S, Tang R, Adams-Huet B, Harris A, Seenivasan T, de Lemos JA, Jialal I. Effect of high-dose α-tocopherol supplementation on biomarkers of oxidative stress and inflammation and carotid atherosclerosis in patients with coronary artery disease. *Am J Clin Nutr.* 2007;86:1392–1398.
14. Gómez-Barrena E, Esteban J, Molina-Manso D, Adames H, Martínez-Morlanes MJ, Terriza A, Yubero F, Puértolas JA. Bacterial adherence on UHMWPE with vitamin E: an in vitro study. *J Mater Sci Mater Med.* 2011;22:1701–1706.
15. Goodman SB, Yao Z, Keeney M, Yang F. The future of biologic coatings for orthopaedic implants. *Biomaterials.* 2013;34:3174–3183.
16. Guralp O. Effects of vitamin E on bone remodeling in perimenopausal women: mini review. *Maturitas.* 2014;79:476–480.
17. Hardes J, Gebert C, Schwappach A, Ahrens H, Streitburger A, Winkelmann W, Gosheger G. Characteristics and outcome of infections associated with tumor endoprostheses. *Arch Orthop Trauma Surg.* 2006;126:289–296.
18. Jiang Q, Yin X, Lill MA, Danielson ML, Freiser H, Huang J. Long-chain carboxychromanols, metabolites of vitamin E, are potent inhibitors of cyclooxygenases. *Proc Natl Acad Sci U S A.* 2008;105:20464–20469.
19. Kamath AF, Ong KL, Lau E, Chan V, Vail TP, Rubash HE, Berry DJ, Bozic KJ. Quantifying the burden of revision total joint arthroplasty for periprosthetic infection. *J Arthroplasty.* 2015;30:1492–1497.
20. Kyomoto M, Shobuike T, Moro T, Yamane S, Takatori Y, Tanaka S, Miyamoto H, Ishihara K. Prevention of bacterial adhesion and biofilm formation on a vitamin E-blended, cross-linked polyethylene surface with a poly(2-methacryloyloxyethyl phosphorylcholine) layer. *Acta Biomater.* 2015;24:24–34.
21. Li D, Gromov K, Søballe K, Puzas JE, O'Keefe RJ, Awad H, Drissi H, Schwarz EM. A quantitative mouse model of implant-associated osteomyelitis and the kinetics of microbial growth, osteolysis and humoral immunity. *J Orthop Res.* 2008;26:96–105.
22. Lorenzetti M, Dogša I, Stošicki T, Stopar D, Kalin M, Kobe S, Novak S. The influence of surface modification on bacterial adhesion to titanium-based substrates. *ACS Appl Mater Interfaces.* 2015;7:1644–1655.
23. Lovati AB, Bottagisio M, de Vecchi E, Gallazzi E, Drago L. Animal models of implant-related low-grade infections. A twenty-year review. *Adv Exp Med Biol.* 2017;971:29–50.
24. Lovati AB, Drago L, Bottagisio M, Bongio M, Ferrario M, Perego S, Sansoni V, De Vecchi E, Romanò CL. Systemic and local administration of antimicrobial and cell therapies to prevent methicillin-resistant *Staphylococcus epidermidis*-induced femoral nonunions in a rat model. *Mediators Inflamm.* 2016;2016:9595706.
25. Lovati AB, Drago L, Monti L, De Vecchi E, Previdi S, Banfi G, Romanò CL. Diabetic mouse model of orthopaedic implant-related *Staphylococcus aureus* infection. *PLoS One.* 2013;8:e67628.
26. Lovati AB, Romanò CL, Bottagisio M, Monti L, De Vecchi E, Previdi S, Accetta R, Drago L. Modeling *Staphylococcus epidermidis*-induced non-unions: subclinical and clinical evidence in rats. *PLoS One.* 2016;11:e0147447.
27. Marko MG, Pang HJ, Ren Z, Azzi A, Huber BT, Bunnell SC, Meydani SN. Vitamin E reverses impaired linker for activation of T cells activation in T cells from aged C57BL/6 mice. *J Nutr.* 2009;139:1192–1197.
28. McCluskey SV. Sterilization of glycerin. *Am J Health Syst Pharm.* 2008;65:1173–1176.
29. Montanaro L, Speziale P, Campoccia D, Ravaioli S, Cangini I, Pietrocola G, Giannini S, Arciola CR. Scenery of *Staphylococcus* implant infections in orthopedics. *Future Microbiol.* 2011;6: 1329–1349.

30. Mueller F, Pfeifer C, Kinner B, Englert C, Nerlich M, Neumann C. Post-traumatic fulminant paradoxical fat embolism syndrome in conjunction with asymptomatic atrial septal defect: a case report and review of the literature. *J Med Case Rep.* 2011;5:142.
31. Naina Mohamed I, Borhanuddin B, Shuid AN, Mohd Fozi NF. Vitamin E and bone structural changes: an evidence-based review. *Evid Based Complement Alternat Med.* 2012;2012:250584.
32. Nazrun AS, Norazlina M, Norliza M, Nirwana SI. The anti-inflammatory role of vitamin E in prevention of osteoporosis. *Adv Pharmacol Sci.* 2012;2012:142702.
33. Negis Y, Aytan N, Ozer N, Ogru E, Libinaki R, Gianello R, Azzi A, Zingg JM. The effect of tocopheryl phosphates on atherosclerosis progression in rabbits fed with a high cholesterol diet. *Arch Biochem Biophys.* 2006;450:63–66.
34. Neuerburg C, Loer T, Mittlmeier L, Polan C, Farkas Z, Holdt LM, Utzschneider S, Schwiesau J, Grupp TM, Böcker W, Aszodi A, Wedemeyer C, Kammerlander C. Impact of vitamin E-blended UHMWPE wear particles on the osseous microenvironment in polyethylene particle-induced osteolysis. *Int J Mol Med.* 2016;38:1652–1660.
35. Pribaz JR, Bernthal NM, Billi F, Cho JS, Ramos RI, Guo Y, Cheung AL, Francis KP, Miller LS. Mouse model of chronic post-arthroplasty infection: noninvasive in vivo bioluminescence imaging to monitor bacterial burden for long-term study. *J Orthop Res.* 2012;30:335–340.
36. Romanò CL, Malizos K, Capuano N, Mezzoprete R, D'Arienzo M, Van Der Straeten C, Scarponi S, Drago L. Does an antibiotic-loaded hydrogel coating reduce early post-surgical infection after joint arthroplasty? *J Bone Jt Infect.* 2016;1:34–41.
37. Romanò CL, Romanò D, Morelli I, Drago L. The concept of biofilm-related implant malfunction and 'low-grade infection.' *Adv Exp Med Biol.* 2017;971:1–13.
38. Romanò CL, Scarponi S, Gallazzi E, Romanò D, Drago L. Antibacterial coating of implants in orthopaedics and trauma: a classification proposal in an evolving panorama. *J Orthop Surg Res.* 2015;10:157.
39. Shiels SM, Bedigrew KM, Wenke JC. Development of a hematogenous implant-related infection in a rat model. *BMC Musculoskelet Disord.* 2015;16:255.
40. Shimazaki T1, Miyamoto H, Ando Y, Noda I, Yonekura Y, Kawano S, Miyazaki M, Mawatari M, Hotokebuchi T. In vivo antibacterial and silver-releasing properties of novel thermal sprayed silver-containing hydroxyapatite coating. *J Biomed Mater Res B Appl Biomater.* 2010;92:386–389.
41. Singh U, Devaraj S. Vitamin E: inflammation and atherosclerosis. *Vitam Horm.* 2007;76:519–549.
42. Takagi S, Chow LC, Hirayama S, Sugawara A. Premixed calcium-phosphate cement pastes. *J Biomed Mater Res B Appl Biomater.* 2003;67:689–696.
43. Tande AJ, Patel R. Prosthetic joint infection. *Clin Microbiol Rev.* 2014;27:302–345.
44. Tiemann A, Hofmann GO, Krukemeyer MG, Krenn V, Langwald S. Histopathological Osteomyelitis Evaluation Score (HOES)–an innovative approach to histopathological diagnostics and scoring of osteomyelitis. *GMS Interdiscip Plast Reconstr Surg DGPW.* 2014;3:Doc08.
45. Voigt J, Mosier M, Darouiche R. Systematic review and meta-analysis of randomized controlled trials of antibiotics and antiseptics for preventing infection in people receiving primary total hip and knee prostheses. *Antimicrob Agents Chemother.* 2015;59:6696–6707.
46. Yang CS, Lu G, Ju J, Li GX. Inhibition of inflammation and carcinogenesis in the lung and colon by tocopherols. *Ann N Y Acad Sci.* 2010;1203:29–34.